AD-A046 636 AERONAUTICAL SYSTEMS DIV WRIGHT-PATTERSON AFB OHIO F/G 21/5
VIBRATIONAL CHARACTERISTICS OF CRACKED CANTILEVER PLATES.(U)
OCT 77 J S OGG
UNCLASSIFIED ASD-TR-77-65 NL

1 OF 1
AD
A046636

END
DATE
FILMED
12-77
DDC

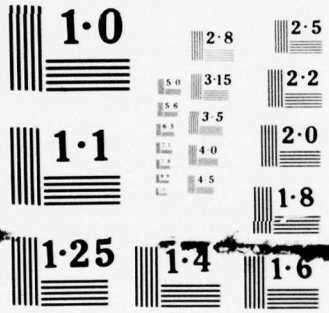

NATIONAL BUREAU OF STANDARDS
MICROCOPY RESOLUTION TEST CHART

AD A046636

ASD-TR-77-65

(12)

VIBRATIONAL CHARACTERISTICS OF CRACKED CANTILEVER PLATES

STRUCTURAL DURABILITY DIVISION
DIRECTORATE OF ENGINEERING AND TEST

D D C
RECEIVED
NOV 28 1977
F

OCTOBER 1977

TECHNICAL REPORT ASD-TR-77-65
Final Technical Report for Period September 1976 – June 1977

AD NO.
DDC FILE COPY

Approved for public release; distribution unlimited.

DEPUTY FOR PROPULSION
AERONAUTICAL SYSTEMS DIVISION
AIR FORCE SYSTEMS COMMAND
WRIGHT-PATTERSON AIR FORCE BASE, OHIO 45433

NOTICE

When Government drawings, specifications, or other data are used for any purpose other than in connection with a definitely related Government procurement operation, the United States Government thereby incurs no responsibility nor any obligation whatsoever; and the fact that the government may have formulated, furnished, or in any was supplied the drawings, specifications, or other data, is not to be regarded by implication or otherwise as in any manner licensing the holder or any other person or corporation, or conveying any rights or permission to manufacture, use, or sell any patented invention that may in any way be related thereto.

This report has been reviewed by the Information Office (OI) and is releasable to the National Technical Information Service (NTIS). At NTIS, it will be available to the general public, including foreign nations.

This technical report has been reviewed and is approved for publication.

JON S. OGG
Aerospace Engineer
Structural Durability Division
ASD/YZES

FOR THE COMMANDER

WESLEY B. CROW, Major, USAF
Chief, Structural Durability Division
Directorate of Engineering & Test
Deputy for Propulsion
ASD/YZES

Copies of this report should not be returned unless return is required by security considerations, contractual obligations, or notice on a specific document.

AIR FORCE/56780/21 November 1977 — 100

UNCLASSIFIED

SECURITY CLASSIFICATION OF THIS PAGE (When Data Entered)

REPORT DOCUMENTATION PAGE

READ INSTRUCTIONS BEFORE COMPLETING FORM

14

1. REPORT NUMBER: ASD-TR-77-65

2. GOVT ACCESSION NO.

3. RECIPIENT'S CATALOG NUMBER

6

4. TITLE (and Subtitle): VIBRATIONAL CHARACTERISTICS OF CRACKED CANTILEVER PLATES.

9

5. TYPE OF REPORT & PERIOD COVERED: Final Technical Report, Sep[redacted]976-June 1977,

6. PERFORMING ORG. REPORT NUMBER

10

7. AUTHOR(s): Jon S. Ogg

8. CONTRACT OR GRANT NUMBER(s)

9. PERFORMING ORGANIZATION NAME AND ADDRESS
Aeronautical Systems Division
Structural Durability Division
Wright-Patterson Air Force Base, Ohio 45433

10. PROGRAM ELEMENT, PROJECT, TASK AREA & WORK UNIT NUMBERS
ASDD-0011

11

11. CONTROLLING OFFICE NAME AND ADDRESS
Aeronautical Systems Division
Directorate of Engineering and Test
Deputy for Propulsion
Wright-Patterson Air Force Base, Ohio 45433

12. REPORT DATE: October 1977

13. NUMBER OF PAGES: 40

14. MONITORING AGENCY NAME & ADDRESS (if different from Controlling Office)

12 50p.

15. SECURITY CLASS. (of this report)

15a. DECLASSIFICATION/DOWNGRADING SCHEDULE

16. DISTRIBUTION STATEMENT (of this Report)
Approved for public release; distribution unlimited.

17. DISTRIBUTION STATEMENT (of the abstract entered in Block 20, if different from Report)

18. SUPPLEMENTARY NOTES

19. KEY WORDS (Continue on reverse side if necessary and identify by block number)
Eigenvalue, Kinetic Energy, Work, Simple Harmonic Oscillation

20. ABSTRACT (Continue on reverse side if necessary and identify by block number)

An analytical solution to the vibrational characteristics of a rectangular cantilever plate with a discontinuous boundary condition (crack) at the root is presented. Mechanical damping which may exist as a result of the contact between the crack's free surfaces during vibration has been eliminated by assuming the crack surface to be a free boundary. The approach to solution involves the use of the method of Ritz applied to Hamilton's Law of Varying Action. A comparison is made to the solution as obtained from conventional

over

DD FORM 1 JAN 73 1473 EDITION OF 1 NOV 65 IS OBSOLETE

UNCLASSIFIED

SECURITY CLASSIFICATION OF THIS PAGE (When Data Entered)

008 800

LB

Block 20 Continued

finite element theory (NASTRAN). No exact solution is available for comparison. The assumptions which underlie both theories are outlined. A comparison is made to the experimental results for a cantilever plate with a narrow slot of varying lengths at the root. Indications are that significant frequency deterioration and nodal pattern variations occur with increasing crack length. Further work on the effect of cracks/flaws on plate response is warranted. The author considers this work a step forward in determining and understanding the effects of flaws/crack on blade response (i.e., high cycle fatigue, flutter) in gas turbine engines today. Further investigation is warranted.

FORWORD

This technical report was prepared in the Directorate of Engineering and Test, Structural Durability Division, Deputy for Propulsion, Aeronautical Systems Division, Wright-Patterson Air Force Base, Ohio. The work was accomplished under ASDD 0011 during the period between September 1976 through May 1977.

J. S. Ogg acknowledges the support of both Dr. James MacBain and his assistant, Bruce Tavner, for their services, thus making the experimental portion of this report possible.

ACCESSION for
NTIS White Section
DDC Buff Section
UNANNOUNCED
JUSTIFICATION
BY
DISTRIBUTION/AVAILABILITY CODES
SPECIAL
A

TABLE OF CONTENTS

SECTION		PAGE
I	INTRODUCTION	1
II	THEORY	4
	1. Strain-Displacement Relationships	
	2. Work	
	3. Kinetic Energy	
	4. Hamilton's Energy Equation	
	5. Plate Coordinate Configuration	
	6. Displacement Functions	
III	RESULTS	14
IV	CONCLUSIONS	17
	APPENDIX Matrix Elements	35
REFERENCES		39

PRECEDING PAGE BLANK-NOT FILMED

LIST OF ILLUSTRATIONS

Figure		Page
1	Cantilever Cracked Plate Coordinate System	21
2	Root Crack Length vs. Eigenvalue Mode 1, AR = 2, ν = .3	22
3	Root Crack Length vs. Eigenvalue Mode 2, AR = 2, ν = .3	22
4	Root Crack Length vs. Eigenvalue Mode 3, AR = 2, ν = .3	23
5	Root Crack Length vs. Eigenvalue Mode 4, AR = 2, ν = .3	23
6	Root Crack Length vs. Eigenvalue Mode 5, AR = 2, ν = .3	24
7	Root Crack Length vs. Eigenvalue Mode 6, AR = 2, ν = .3	24
8	Root Crack Length vs. Eigenvalue Mode 7, AR = 2, ν = .3	25
9	Root Crack Length vs. Eigenvalue Mode 8, AR = 2, ν = .3	25
10	Vibration Nodal Patterns Mode 1, AR = 2, ν = .3	26
11	Vibration Nodal Patterns Mode 2, AR = 2, ν = .3	27
12	Vibration Nodal Patterns Mode 3, AR = 2, ν = .3	28
13	Vibration Nodal Patterns Mode 4, AR = 2, ν = .3	29
14	Vibration Nodal Patterns Mode 5, AR = 2, ν = .3	30
15	Vibration Nodal Patterns Mode 6, AR = 2, ν = .3	31

LIST OF ILLUSTRATIONS (CONTINUED)

Figure		Page
16	Vibration Nodal Patterns Mode 7, AR = 2, ν = .3	32
17	Eigenvalue Ratio Deviations from Experimental Solution	33

LIST OF TABLES

Table		Page
1	Uniform Cantilever Plate Eigenvalues	18
2	Eigenvalue Convergence: 2 Element Uniform	19
3	Eigenvalue Convergence: 2 Element Uniform Number of Terms in Truncated Power Series	20

SYMBOLS

A_{ij}, B_{ij}	Unknown coefficient of assumed deflection functions
AR_1, AR_2, AR	Aspect ratios of plate element 1, element 2, and combined elements, respectively
a	Spanwise length of cantilever plate
b_1, b_2	Width of plate elements 1 and 2, respectively
D	Bending stiffness parameter $Eh^3/12(1-\nu^2)$
E	Young's Modulus
h	Plate thickness
i, j, k, ℓ	Subscripts indicating element indicies
$\bar{m}$	Mass per unit area
M, N	Integers which relate to the number of terms in the truncated power series
$\mathbb{K}$, $\mathbb{M}$	Plate stiffness and mass matrices
q_i	Generalized coordinate
t	Independent variable time
T	Kinetic energy
u, v, w	Displacements of plate in the x, y, z directions, respectively, independent of time
W	Work
$\bar{w}$	Displacement of plate in x direction; time dependent

SYMBOLS

$\dot{w}$	Differentiation with respect to time
x, y, z	Orthogonal cartesian coordinates; when used as subscripts, they denote partial differentiation
α	Plate element's width ratio b_1/b_2
δ	Variational operator
$\varepsilon_x, \varepsilon_y, \gamma_{xy}$	Strains in body: bending and shearing
η, ξ	Nondimensional coordinates for y and x directions; when used as subscripts, they represent partial differentiation
λ	Frequency parameter: plate eigenvalue
ν	Poisson's Ratio
ρ	Mass density
Σ	Summation
$\sigma_x, \sigma_y, \tau_{xy}$	Stresses in body: bending and shearing
ϕ, θ	Geometric boundary constraint parameters
ω	Natural frequency of vibrating system
∂	Partial differential operator

SECTION I

INTRODUCTION

At the present time, a great deal of attention is being directed to turbine engine structural durability. Emphasis is now placed on either extending or extracting the maximum useful life from engine hardware. With major advances being made in fracture mechanics, the day may soon arrive when an engine's structural components will be designed to satisfy a damage tolerance criteria similar to that employed on airframes today. Therefore, total understanding of the effect of discrepancies, i.e., flaws and cracks on engine hardware, is necessary before such an approach to design can be feasible.

One area which may be especially sensitive to these discrepancies is turbine engine blades (i.e., fan, compressor, and turbine). Engines are designed to meet certain requirements which are determined by blade response (i.e., flutter boundaries, engine order blade excitations, etc.). Both blade flutter and frequency response are dependent upon material and mechanical damping characteristics, blade mode shapes, and natural frequencies of excitation. This paper will explore the effects of cracks on the mode shapes and frequencies of blades. For the purpose of portraying the relative effects of cracks, a flat plate with an aspect ratio of two will serve as the blade model for this investigation.

Much work has been directed to the solution of the flat plate vibration problem. Extensive documentation (Reference 1) of upper and

lower bounds of solutions for various plate geometrics has meticulously defined what the exact value of solution would be, provided it could be obtained. Various techniques to solution have been employed yielding reasonable accuracy, however, no exact solution is available for the nonuniform (cracked) boundary value problem. Probably one of the most powerful tools for the solution of a problem of this nature is that of the finite element theory. The utility of such an approach to solution is questionable when a more direct, simplified, and economical means of solution is available; namely, the energy solution. It is unfortunate that some energy approaches to solutions (i.e., Rayleigh, Galerkin) have masked the power of this type of approach. The major drawback of these approaches has been the need of selecting "appropriate" shape functions which satisfy the geometrical constraints and approximate the modes of vibration. The accuracy of the solutions are primarily dependent on these assumed functions. Ritz (Reference 2) demonstrated that through the use of a truncated series, properly employed, an upper bound on the true solution to deformable body problems could be obtained. The benefits of using an approach to solution as eluded to by Ritz can best be summarized as follows (Reference 3). "Advantages of the Ritz method lie in the relative ease with which complex boundary conditions can be handled. It is a powerful tool yielding high accuracy in the deflection analysis . . . The Ritz method can be considered as one of the most usable methods of higher analysis for solving complex boundary value problems in the mathematical physics." The relative ease and accuracy of this approach combined with the concepts

associated with Hamilton's Law of Varying Action provides an analytical means of solution for a wide range of applications (i.e., conservative, nonconservative, stationary, and nonstationary motion of particles, beams, plates and shells (References 4 through 8).

This paper will concentrate on the stationary motion of the simple harmonic vibration of thin flat plates. Since no in-plane vibrations (membrane) will be considered, the out-of-plane deflection w can be written as a function of the in-plane coordinates x, y, and time, t. As will be shown, the assumptions associated with linear, plane stress solutions may no longer be valid to solve a highly nonuniform vibration problem such as in the crack plate response.

SECTION II

THEORY

It is often difficult to determine which equation will yield the best results when solving a particular problem using an energy approach. Therefore, it is best to start with the most fundamental equation which encompasses all other energy approaches to solution. Such an equation was postulated by Sir William Rowan Hamilton and was called by him the "Law of Varying Action" (Reference 9). It can be mathematically stated as,

$$\delta \int_{t_0}^{t_1} (T + W)\, dt - \frac{\partial T}{\partial \dot{q}_i} \delta q_i \Big|_{t_0}^{t_1} = 0 \qquad (1)$$

where T represents the total kinetic energy of the system and W is the total work of the forces acting on or within the system.

1. STRAIN-DISPLACEMENT RELATIONSHIPS

For the purpose of this analysis, the plate is considered to be composed of an isotropic continuum which obeys the elastic stress-strain relationships. In addition, the assumptions underlying thin plate theory (plane stress) are assumed valid for the vibrational analysis. From this assumption we have,

$$\tau_{yz} = \tau_{zx} = \sigma_z = 0$$

which reduces the stress-strain relationships to,

$$\sigma_x = \frac{E}{(1 - \nu^2)} \quad (\varepsilon_x + \nu\varepsilon_y)$$

$$\sigma_y = \frac{E}{(1 - \nu^2)} \quad (\varepsilon_y + \nu\varepsilon_x) \tag{2}$$

$$\tau_{xy} = \frac{E}{2(1 + \nu)} \quad (\gamma_{xy})$$

Membrane stresses have not been considered for this analysis (inextensional plate theory) since there are no externally applied (thermal or mechanical) in-plane loads. From the assumption of small deflections during vibration, the corresponding strain-displacement equations reduce to a set of linear equations of the form,

$$\varepsilon_x = \frac{\partial u}{\partial x}$$

$$\varepsilon_y = \frac{\partial v}{\partial y} \tag{3}$$

$$\gamma_{xy} = \frac{\partial v}{\partial x} + \frac{\partial u}{\partial y}$$

With the two assumptions, plane stress and small deflections, the in-plane displacements, u, v, can be expressed as functions of the out-of-plane deflection, w.

$$u = -z \frac{\partial \bar{w}}{\partial x}$$

$$v = -z \frac{\partial \bar{w}}{\partial y} \tag{4}$$

Substituting Equations 4 into Equations 3 and combining with Equations 2 yields,

$$\sigma_x = \frac{E}{(1 - \nu^2)} \left(-z \frac{\partial^2 \bar{w}}{\partial x^2} - \nu z \frac{\partial^2 \bar{w}}{\partial y^2} \right)$$

$$\sigma_y = \frac{E}{(1 - \nu^2)} \left(-z \frac{\partial^2 \bar{w}}{\partial y^2} - \nu z \frac{\partial^2 \bar{w}}{\partial x^2} \right) \tag{5}$$

$$\tau_{xy} = \frac{E}{2(1 + \nu)} \left(-2z \frac{\partial^2 \bar{w}}{\partial x \partial y} \right)$$

2. WORK

For the conservative, stationary problem of the free vibration where there are no external forces, the work of the internal stresses may be expressed as the volume integral of the strain energy density function,

$$W = -\frac{1}{2} \iiint (\sigma_x \varepsilon_x + \sigma_y \varepsilon_y + \tau_{xy} \gamma_{xy}) \, dx \, dy \, dz \tag{6}$$

3. KINETIC ENERGY

The contribution of rotary inertia to the total kinetic energy has been found to be insignificant for small vibrations of a thin

plate. Therefore, the kinetic energy can be expressed as,

$$T = \frac{1}{2}\iiint \rho\dot{\bar{w}}^2 \, dx \, dy \, dz \tag{7}$$

As a result of ρ, w, $\dot{w}$ satisfying natural continuity conditions within the region occupied by the plate material,

$$\frac{\partial T}{\partial \dot{q}_i} \delta q_i \Big|_{t_0}^{t_1} = \iiint \rho\dot{\bar{w}}\delta\bar{w} \, dxdydz \Big|_{t_0}^{t_1} \tag{8}$$

Taking the variation of Equation 7 and combining with Equation 8, as in Hamilton's Law,

$$\int_{t_0}^{t_1} \delta T \, dt - \frac{\partial T}{\partial \dot{q}_i} \delta q_i \Big|_{t_0}^{t_1} = \int_{t_0}^{t_1}\left[\iiint \rho\dot{\bar{w}}\delta\dot{\bar{w}} \, dx \, dy \, dz\right] \cdot dt - \iiint \rho\dot{\bar{w}}\delta\bar{w} \, dx \, dy \, dz \Big|_{t_0}^{t_1} \tag{9}$$

Integrating the first term of Equation 9 by parts with respect to time and carrying out the necessary algebraic operations yields,

$$-\int_{t_0}^{t_1}\left[\iiint \rho\ddot{\bar{w}}\delta\bar{w} \, dx \, dy \, dz\right] \cdot dt \tag{10}$$

4. HAMILTON'S ENERGY EQUATION

Substituting Equations 6 and 10 into Equation 1, Hamilton's Law, results in the time integral of the principle of virtual work,

$$\int_{t_0}^{t_1} \left[-\iiint_V \rho \ddot{\bar{w}} \delta \bar{w} dxdydz - \iiint_V (\sigma_x \delta \varepsilon_x + \sigma_y \delta \varepsilon_y + \tau_{xy} \delta \gamma_{xy})\, dxdydz \right] \tag{11}$$

$$dt = 0$$

The resulting equation within the time integral in terms of the displacements of the system under consideration is well known,

$$\int_{t_0}^{t_1} \left[- \iint_A D \left\{ \frac{\partial^2 \bar{w}}{\partial x^2} \delta \frac{\partial^2 \bar{w}}{\partial x^2} + \frac{\partial^2 \bar{w}}{\partial y^2} \delta \frac{\partial^2 \bar{w}}{\partial y^2} + \nu \frac{\partial^2 \bar{w}}{\partial x^2} \delta \frac{\partial^2 \bar{w}}{\partial y^2} + \nu \frac{\partial^2 \bar{w}}{\partial y^2} \delta \frac{\partial^2 \bar{w}}{\partial x^2} + \right. \tag{12}$$

$$\left. 2 \cdot (1 - \nu) \frac{\partial^2 \bar{w}}{\partial x \partial y} \delta \frac{\partial^2 \bar{w}}{\partial x \partial y} \right\} dxdy - \bar{m} \iint_A \ddot{\bar{w}} \delta \bar{w}\, dxdy \right] dt = 0$$

Assuming simple harmonic motion of the vibrating plate (free vibration), the displacement, w, can be expressed as,

$$\bar{w}(x,y,t) = w(x,y) \sin \omega t \tag{13}$$

Substituting this expression into Equation 12 and collecting terms yields,

$$\left[\omega^2 \iint_A \bar{m} w \delta w dxdydz - \iint D \left\{ \frac{\partial^2 w}{\partial x^2} \delta \frac{\partial^2 w}{\partial x^2} + \frac{\partial^2 w}{\partial y^2} \delta \frac{\partial^2 w}{\partial y^2} + \right. \right.$$

$$\left. \left. \nu \frac{\partial^2 w}{\partial y^2} \delta \frac{\partial^2 w}{\partial x^2} + \nu \frac{\partial^2 w}{\partial x^2} \delta \frac{\partial^2 w}{\partial y^2} + 2(1 - \nu) \frac{\partial^2 w}{\partial x \partial y} \delta \frac{\partial^2 w}{\partial x \partial y} \right\} dxdy \right] \cdot \tag{14}$$

$$\int \sin^2 \omega t dt = 0$$

Recognizing that the integral

$$\int_{t_0}^{t_1} \sin^2 \omega t dt$$

cannot vanish for any time, t_1, larger than t_0, implies that the following condition must exist.

$$\omega^2 \iint_A \bar{m} w \delta w dxdy - \iint D \left\{ \frac{\partial^2 w}{\partial x^2} \delta \frac{\partial^2 w}{\partial x^2} + \frac{\partial^2 w}{\partial y^2} \delta \frac{\partial^2 w}{\partial y^2} + \nu \frac{\partial^2 w}{\partial x^2} \delta \frac{\partial^2 w}{\partial y^2} + \right.$$

$$\left. \nu \frac{\partial^2 w}{\partial y^2} \delta \frac{\partial^2 w}{\partial x^2} + 2(1 - \nu) \frac{\partial^2 w}{\partial x \partial y} \delta \frac{\partial^2 w}{\partial x \partial y} \right\} dxdy = 0 \qquad (15)$$

Equation 15, as derived is applicable to only simple harmonic motion of the system.

5. PLATE COORDINATE CONFIGURATION

To aid in satisfying the necessary boundary conditions, the plate has been modeled as two discrete elements, one of which embodies the free surface of the crack. The coordinate system used for the analysis of the combined plate elements is shown in Figure 1. Dimensional characteristics of the elements served to model the root crack configuration for a series of crack depths (% chord). The nondimensionalization performed consisted of the following:

$$\eta_1 = \eta_2 = y/a \qquad \xi_1 = x_1/b_1 \qquad \xi_2 = x_2/b_2$$

$$dy_1 = dy_2 = a d\eta \qquad dx_1 = b_1 d\xi_1 \qquad dx_2 = b_2 d\xi_2$$

$$AR_1 = a/b_1 \qquad\qquad AR_2 = a/b_2$$

$$\text{Combined Plate AR} = \frac{AR_1 \cdot AR_2}{AR_1 + AR_2}$$

6. DISPLACEMENT FUNCTIONS

Based on the concepts as defined by Ritz (Reference 2) and knowledge gained from References 4 through 8, a set of admissable functions in the form of a simple truncated power series served as the deflection function for this analysis. The functions used for solving the crack plate problem are expressed in the nondimensional form,

$$W_1(\xi_1, \eta) = g_1(\xi_1, \eta) \sum_{j=0}^{N} \sum_{i=0}^{M} A_{ij} \eta^i \xi_1^j$$

$$W_2(\xi_2, \eta) = g_2(\xi_2, \eta) \sum_{j=0}^{N} \sum_{i=0}^{M} B_{ij} \eta^i \xi_2^j \tag{16}$$

where the term $g(\xi, \eta)$ forces satisfaction of the prescribed geometrical boundary conditions. The most general form of this function for the coordinate system, Figure 1, chosen is, Fig 1

$$g(\xi,\eta) = \xi^{\phi_1}(1 - \xi)^{\phi_2}\eta^{\theta_1}(1 - \eta)^{\theta_2} \tag{17}$$

The specific values of the ϕs and θs in Equation 17 for the two element solution are,

Element 1: $\theta_1 = 2 \qquad \phi_1 = \phi_2 = \theta_2 = 0$

Element 2: $\phi_1 = \phi_2 = \theta_1 = \theta_2 = 0$ (18)

For the line of commonality between the two elements the following continuity conditions are required,

Displacement: $W_1\ (1, \eta) = W_2\ (0, \eta)$

Chordwise Slope: $W_{1_x}\ (1, \eta) = W_{2_x}\ (0, \eta)$ (19)

Spanwise Slope: $W_{1_y}\ (1, \eta) = W_{2_y}\ (0, \eta)$

The author's experience (Reference 8) in performing these types of calculations for the case of beams with discontinuities has shown that satisfying only the slope and displacement conditions along the connecting boundary has provided excellent convergence on the higher order derivatives corresponding to the moments, shears, and forces. Satisfying the three continuity requirements, Equations 19, and substituting the appropriate "g" functions, Equation 18, into Equations 16 yields,

$$W_1\ (\xi_1, \eta) = \sum_{j=0}^{N} \sum_{i=0}^{M} A_{ij}\ \eta^{i + 2}\xi^{j}$$

$$W_2(\xi_2, \eta) = \sum_{j=0}^{N}\sum_{i=0}^{M} A_{ij}\,\eta^{i+2} + \alpha\sum_{j=0}^{N}\sum_{i=0}^{M} A_{ij}(j)\eta^{i+2}\xi_2 + \sum_{j=2}^{N}\sum_{i=0}^{M} B_{ij}\eta^{i}\xi_2^{j} \tag{20}$$

Replacing the deflection functions in Equations 18 with Equations 20 and performing the necessary operation with the operator, δ, where

$$\delta W_1 = \sum_{\ell=0}\sum_{k=0} \eta^{k+2}\xi^{\ell}\delta A_{k\ell}$$

$$\delta W_2 = \sum_{\ell=0}^{N}\sum_{k=0}^{M} \eta^{k+2}\delta A_{k\ell} + \alpha\sum_{\ell=0}^{N}\sum_{k=0}^{M} \ell\eta^{k+2}\xi_2 A_{k\ell} + \sum_{\ell=2}^{N}\sum_{k=0}^{M} \eta^{k}\xi_2^{\ell}\delta B_{k\ell}$$

results in the set of equations of the form,

$$\sum_{j=0}^{N}\sum_{i=0}^{M} A_{ij}\left[(K1_{ijk\ell} - \lambda^2 M1_{ijk\ell}) + B_{ij}\,(K2_{i\bar{j}k\ell} - \lambda^2 M2_{i\bar{j}k\ell})\right] = 0 \tag{21}$$

for $k = 0, 1, 2 \ldots M$

$\ell = 0, 1, 2 \ldots N$

$\bar{j} = 2, 3 \ldots N$

$$\sum_{j=0}^{N}\sum_{i=0}^{M}\left[A_{ij}\left(K2^{T}_{ijk\bar{\ell}} - \lambda^{2}M^{T}2_{ijk\bar{\ell}}\right) + B_{ij}\left(K3_{i\bar{j}k\bar{\ell}} - \lambda^{2}M3_{i\bar{j}k\bar{\ell}}\right)\right] = 0 \tag{22}$$

for $k = 0, 1, 2 \ldots M$

$\bar{j} = 2, 3 \ldots N$

$\bar{\ell} = 2, 3 \ldots N$

The recursion formulas for the matrix elements are presented in the Appendix. Equations 21 and 22 can be expressed in matrix form as,

$$\left[\underbrace{\begin{bmatrix} [K1] & [K2] \\ [K2]^{T} & [K3] \end{bmatrix}}_{\mathbb{K}} - \lambda^{2}\underbrace{\begin{bmatrix} [M1] & [M2] \\ [M2]^{T} & [M3] \end{bmatrix}}_{\mathbb{M}}\right]\begin{Bmatrix} A \\ B \end{Bmatrix} = 0 \tag{23}$$

The $\mathbb{K}$ and $\mathbb{M}$ are square symmetric matrices of order $M \cdot (2N - 2)$. For a nontrivial solution to this set of homogeneous equations, the determinant of the coefficient matrix must vanish.

$$\left|[\mathbb{K}] - \lambda^{2}[\mathbb{M}]\right| = 0 \tag{24}$$

SECTION III

RESULTS

Before attempting the solution to the nonuniform cantilever plate problem using the method of Ritz, a study of the rate and type of convergence possible was performed. The uniform cantilever plate vibration problem served to demonstrate the convergence possible using this approach. A great deal of data, both experimental and analytical, was available for comparison. Table 1 summarizes the eigenvalue comparisons for the various solution schemes.

A convergence study was conducted for the uncracked configuration on the effects of varying the aspect ratios of the two separate elements while maintaining the same combined aspect ratio of 2. Table 2 summarizes the results of this study for four different element combinations. As depicted, little variation was noted for the cases considered. In addition, Table 3 shows the results of a study conducted on the rate of eigenvalue convergence as a function of the number of terms used in the truncated power series. A study of this type was not performed on the effect of the number of elements in the finite element solution due to cost restraints. The average cost of extracting approximately 84 eigenvalues and their corresponding eigenvectors using the direct approach was $15.00. However, the cost of extracting the first 10 eigenvalues and mode shapes using the finite element program, NASTRAN, was $150.00. A study was performed and documented (Reference 10) which showed a sufficient lower bound convergence for a rectangular cantilever plate with an aspect ratio of 2 using the

same number and type of finite elements. In all cases, good agreement was obtained for the uniform cantilever plate solution schemes, Ritz, and finite element when compared to experimental and other analytical solutions.

With the good correlation between the experimental, direct, and finite element solutions for the uniform plate, the problem of the mixed boundary condition plate response was addressed. The crack was introduced into the analytical solutions as a free boundary with no surface interactions. For the experimental test, a narrow cut was made along the root of the plate attachment. The plate was not removed from its support throughout the entire testing sequence. An acoustical siren served as the excitation source. Resonant conditions were defined by two separate methods.

One approach employed the use of a laser interferometry technique to visually detect the resonant mode through the laser light interference patterns. The second method involved the use of an oscilloscope and a piezo-electric accelerometer. Resonant conditions were determined by plotting the input forcing function (sinusoidal) against the output signal as relayed by the accelerometer. The plate used for obtaining the experimental data consisted of an aluminum flat plate 1/8" x 3" x 6" rigidly constrained at one edge by two solid steel blocks. These blocks were attached to an air-damped (floating) table. Poisson's ratio (ν) of 0.3, mass density of 0.100 lb/in^3, and elastic modules (E)

of 1.0×10^7 lbf/in^2 were assumed for the analytical portion of the study.

Figures 2 through 9 portray the eigenvalue results for the first eight out-of-plane vibration modes. The data depicts the response as a function of root crack length for the three solution schemes. All eigenvalues have been normalized to the uniform (uncracked) configuration corresponding to each solution. In all cases, the experimental frequencies fall below the two analytical solutions. Reasonably good agreement can be seen in most instances between the finite element and energy solutions. In addition, Figures 10 through 16 show the variation in mode shapes as a function of crack length. The experimental mode shapes consist of the holograms taken from the laser setup previously mentioned. The finite element mode shape plots are contour surface diagrams, whereas the energy solution generated plots represent positive and negative out-of-plane displacements.

SECTION IV

CONCLUSIONS

The results of this work have demonstrated that a direct and economical solution to the nonuniform plate vibration can be obtained. Excellent agreement was shown for the uniform plate vibration solution when compared to those obtained from literature. Comparison of the results for the nonuniform vibration problem has indicated some differences between the theoretical and experimental solutions. Similar results were obtained for both the finite element and energy solutions. Figure 17 portrays the relative comparison between the uniform and nonuniform deviations from the experimental solution. As shown, a marked increase in the percent difference occurs for the cracked plate solution. This difference may possibly be explained by either a breakdown in the assumptions associated with thin plate vibration theory or the approach used in obtaining the experimental results. Both results indicate the same type of frequency decay with increasing crack length, but differ slightly in the absolute value of this decay. Additional experimental testing and analysis are necessary to resolve the problem of the noted difference.

This paper has presented an essential step towards the understanding of the effect of cracks on quasi-blade response. It is apparent from the results that further work in the area of nonuniform blade response is warranted before consideration is given to extending the damage tolerance criteria to gas turbine engine airfoils.

TABLE 1. UNIFORM CANTILEVER PLATE EIGENVALUES

AR= 2.0 = .3

MODE NO.	$\lambda^2 = m l^4 \omega^2 / D$					
	Direct Soln. 1 Element Ogg	Direct Soln. 2 Element Ogg	Finite Element Soln. 160 Elem. NASTRAN	Exper'l Soln. Leissa [Ref.1]	Exper'l Soln. Ogg	Exper'l Soln. Leissa [Ref. 1]
1	11.835	11.846	11.806	12.250	11.056	12.055
2	219.208	219.283	214.458	210.250	203.028	222.905
3	459.653	459.927	455.511	470.890	431.177	466.992
4	2322.321	2323.173	2263.561	2313.610	2145.366	2372.664
5	3619.635	3623.269	3567.303	3660.250	3141.098	——

TABLE 2. EIGENVALUE CONVERGENCE: 2 ELEMENT UNIFORM

$$AR = \frac{AR_1 \cdot AR_2}{AR_1 + AR_2} = 2.0 \qquad = .3$$

MODE NO.	$\lambda^2 = m l^4 \omega^2 / D$			
	$AR_2 = 16.00$, $AR_1 = 2.28$	$AR_2 = 8.00$, $AR_1 = 2.66$	$AR_2 = 5.35$, $AR_1 = 3.20$	$AR_2 = 4.00$, $AR_1 = 4.00$
1	11.846	11.846	11.846	11.846
2	219.286	219.284	219.283	219.283
3	459.930	459.930	459.930	459.930
4	2323.216	2323.191	2323.183	2323.178
5	3623.289	3623.280	3623.273	3623.271
6	8570.865	8570.664	8570.610	8570.589
7	8670.115	8670.064	8670.018	8670.000

TABLE 3. EIGENVALVE CONVERGENCE: 2 ELEMENT UNIFORM

NUMBER OF TERMS OF TRUNCATED POWER SERIES $\sum_{j=0}^{N} \sum_{i=0}^{M} (- - - - -) + \sum_{j=2}^{N} \sum_{i=0}^{M} (- - - - -)$

MODE NO.	$\lambda^2 = m l^4 \omega^2 / D$				
	N=M=5 (40)	Δ (%)	N=M=6 (60)	Δ (%)	N=M=7 (84)
1	11.881	0.20	11.857	0.09	11.846
2	219.475	0.05	219.359	0.03	219.283
3	460.580	0.08	460.196	0.06	459.929
4	2326.473	0.12	2323.685	0.02	2323.178
5	3809.110	5.00	3624.719	0.04	3623.271
6	8732.285	1.90	8573.075	0.03	8570.589
7	8850.409	1.90	8679.997	0.11	8669.999

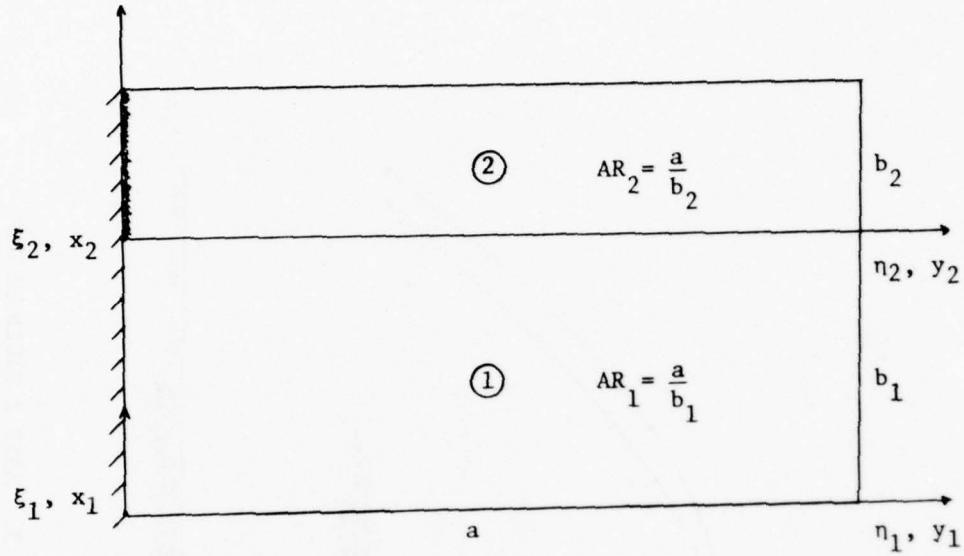

$$AR = \frac{AR_1 \quad AR_2}{AR_1 + AR_2}$$

$$\eta_1 = \eta_2 = \eta = \frac{y}{a}$$

$$\eta_1 = \frac{x_1}{b_1}$$

$$\eta_2 = \frac{x_2}{b_2}$$

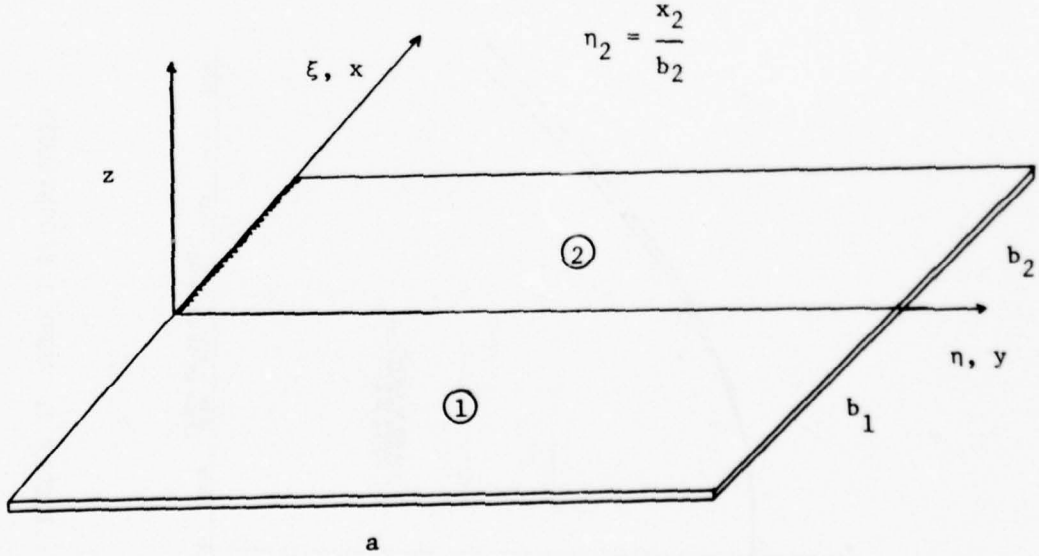

FIGURE 1. CANTILEVER CRACKED PLATE COORDINATE SYSTEM

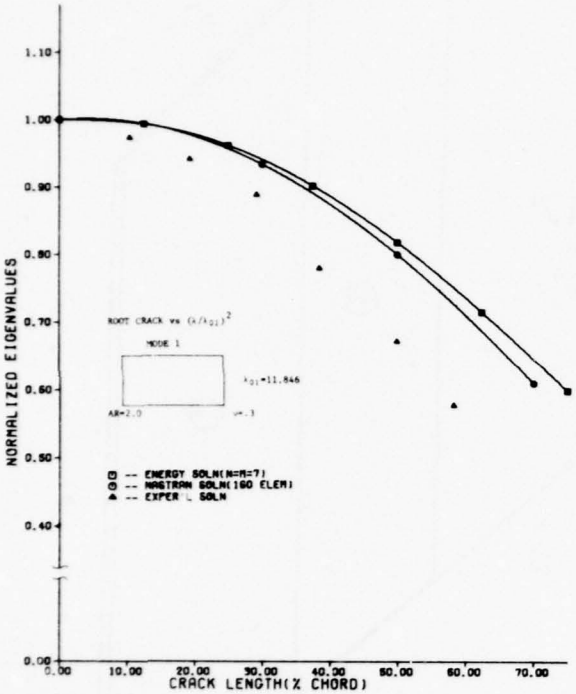

FIGURE 2. MODE 1 EIGENVALUES

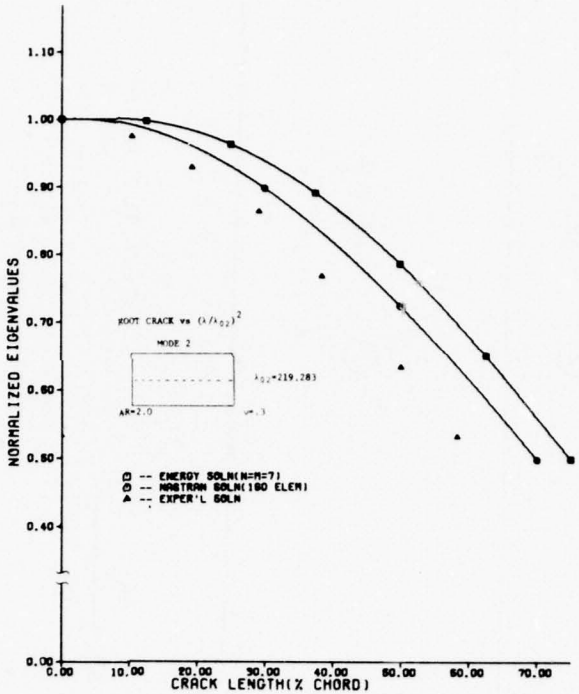

FIGURE 3. MODE 2 EIGENVALUES

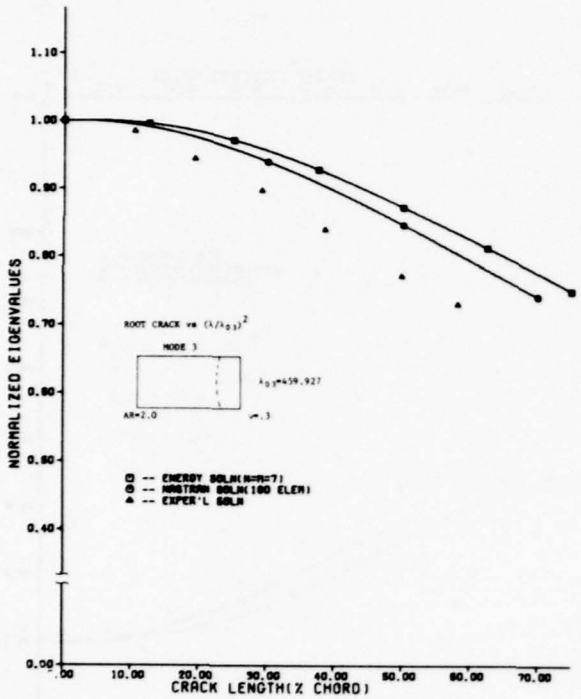

FIGURE 4. MODE 3 EIGENVALUES

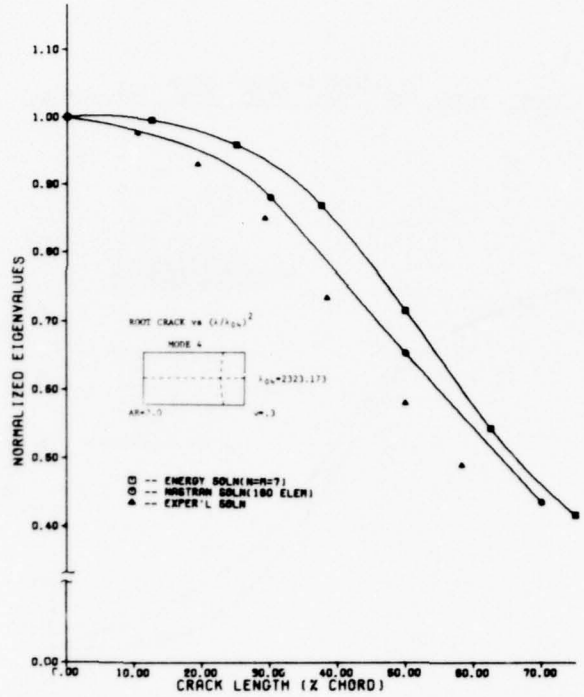

FIGURE 5. MODE 4 EIGENVALUES

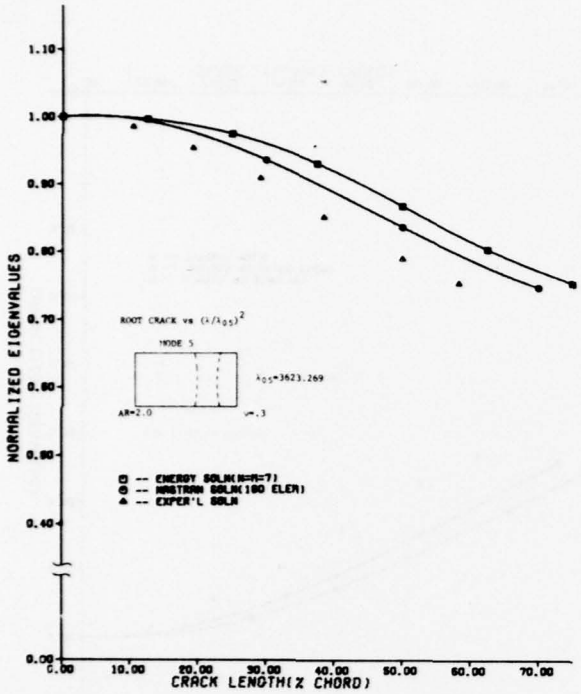

FIGURE 6. MODE 5 EIGENVALUES

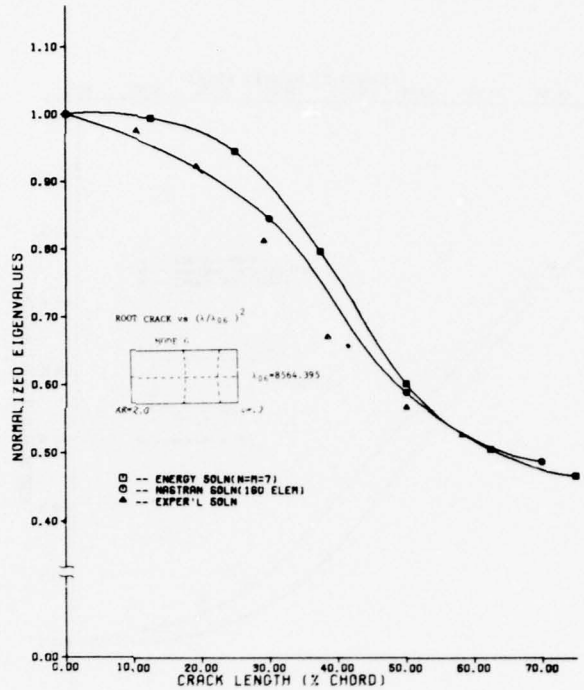

FIGURE 7. MODE 6 EIGENVALUES

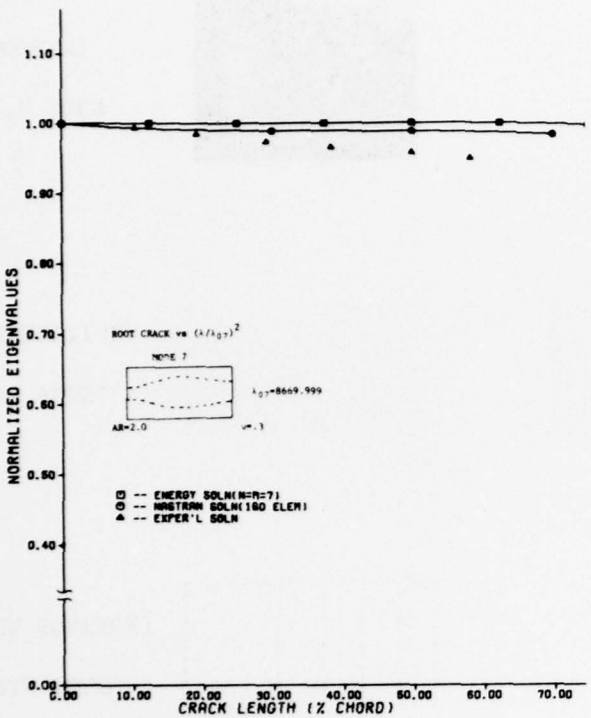

FIGURE 8. MODE 7 EIGENVALUES

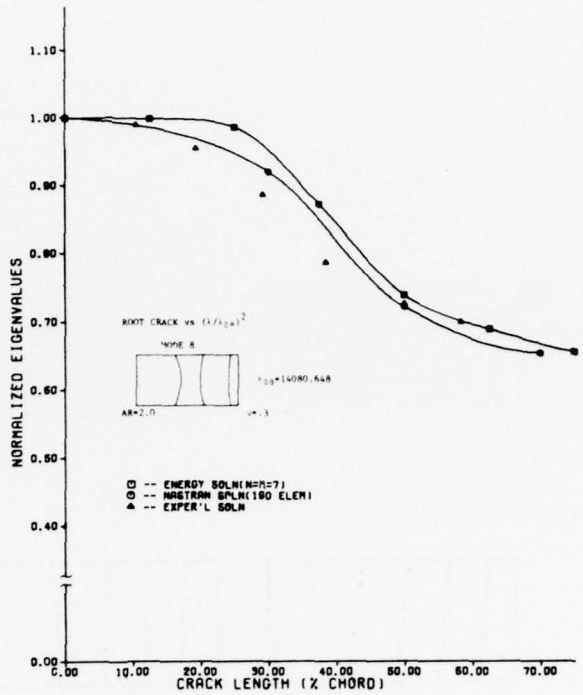

FIGURE 9. MODE 8 EIGENVALUES

ROOT CRACK LENGTH (% CHORD)

0.0 .... 10.0 .... 20.0 .... 30.0 .... 40.0 .... 50.0 .... 60.0 .... 70.0

NASTRAN SOLN.

(CONTOUR SURFACE)

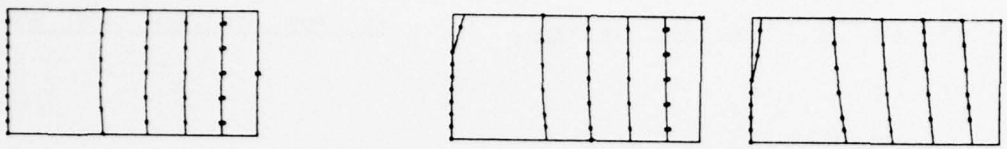

ENERGY SOLN.

(± DEFLECTION)

EXPER'L SOLN.

(HOLOGRAM)

FIGURE 10. ROOT CRACK MODE SHAPE: MODE 1

ROOT CRACK LENGTH (% CHORD)

0.0 .... 10.0 .... 20.0 .... 30.0 .... 40.0 .... 50.0 .... 60.0 .... 70.0

NASTRAN SOLN.

(CONTOUR SURFACE)

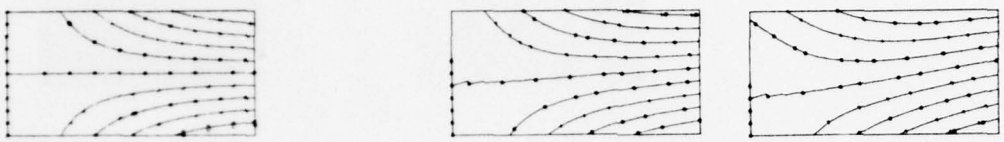

ENERGY SOLN.

(± DEFLECTION)

EXPER'L SOLN.

(HOLOGRAM)

FIGURE 11. ROOT CRACK MODE SHAPE: MODE 2

ROOT CRACK LENGTH (% CHORD)

0.0 .... 10.0 .... 20.0 .... 30.0 .... 40.0 .... 50.0 .... 60.0 .... 70.0

NASTRAN SOLN.

(CONTOUR SURFACE)

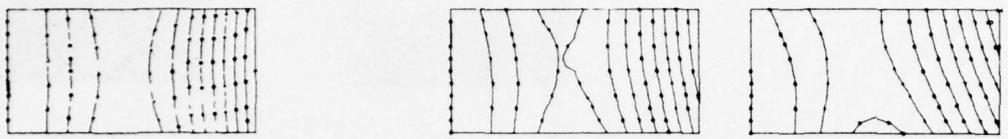

ENERGY SOLN.

(± DEFLECTION)

EXPER'L SOLN.

(HOLOGRAM)

FIGURE 12. ROOT CRACK MODE SHAPE: MODE 3

ROOT CRACK LENGTH (% CHORD)

0.0 .... 10.0 .... 20.0 .... 30.0 .... 40.0 .... 50.0 .... 60.0 .... 70.0

NASTRAN SOLN.

(CONTOUR SURFACE)

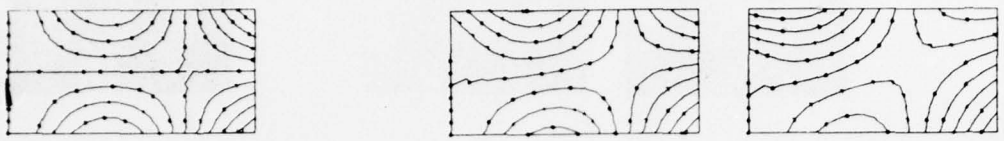

ENERGY SOLN.

(± DEFLECTION)

EXPER'L SOLN.

(HOLOGRAM)

FIGURE 13. ROOT CRACK MODE SHAPE: MODE 4

ROOT CRACK LENGTH (% CHORD)

0.0 .... 10.0 .... 20.0 .... 30.0 .... 40.0 .... 50.0 .... 60.0 .... 70.0

NASTRAN SOLN.

(CONTOUR SURFACE)

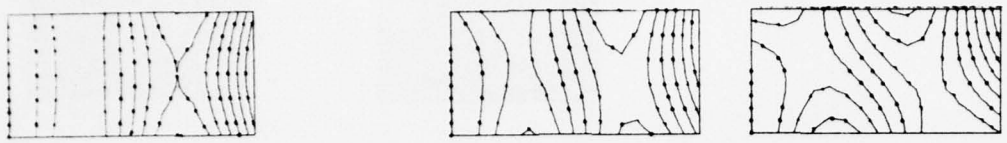

ENERGY SOLN.

(± DEFLECTION)

EXPER'L SOLN.

(HOLOGRAM)

FIGURE 14. ROOT CRACK MODE SHAPES: MODE 5

ROOT CRACK LENGTH (% CHORD)

0.0 .... 10.0 .... 20.0 .... 30.0 .... 40.0 .... 50.0 .... 60.0 .... 70.0

NASTRAN SOLN.

(CONTOUR SURFACE)

ENERGY SOLN.

(± DEFLECTION)

EXPER'L SOLN.

(HOLOGRAM)

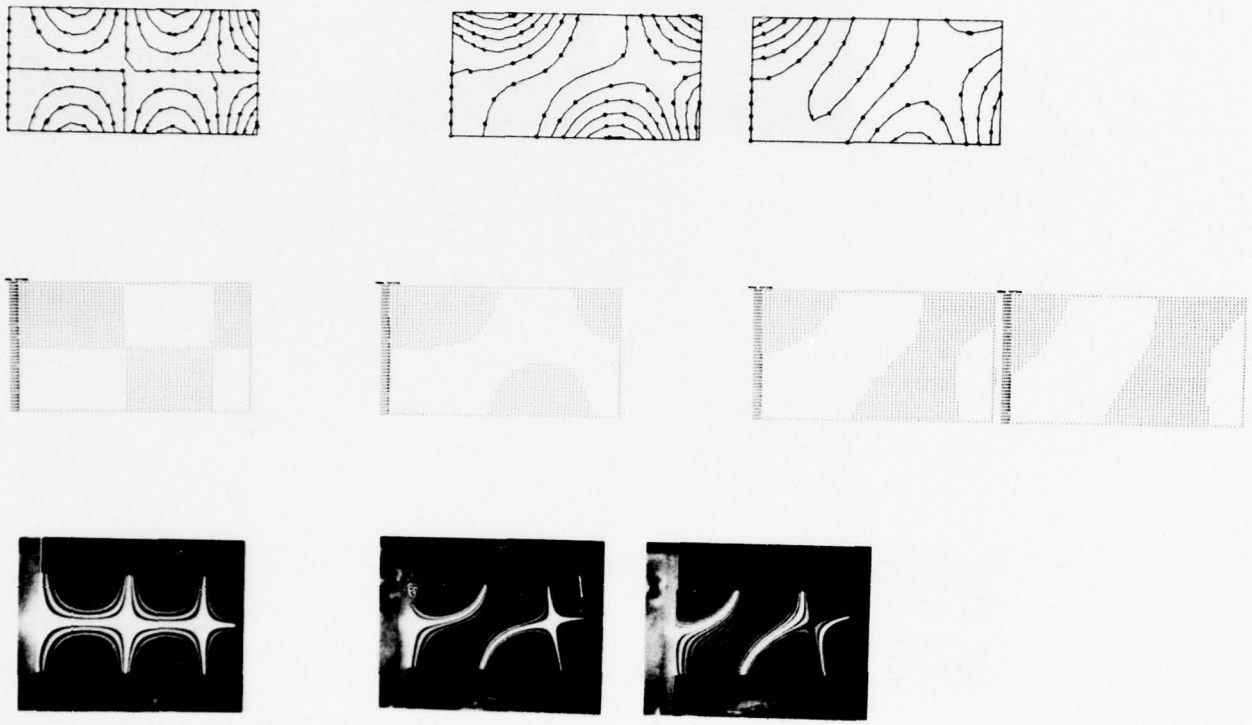

FIGURE 15. ROOT CRACK MODE SHAPES: MODE 6

ROOT CRACK LENGTH (% CHORD)

0.0 .... 10.0 .... 20.0 .... 30.0 .... 40.0 .... 50.0 .... 60.0 .... 70.0

NASTRAN SOLN.

(CONTOUR SURFACE)

ENERGY SOLN.

(± DEFLECTION)

EXPER'L SOLN.

(HOLOGRAM)

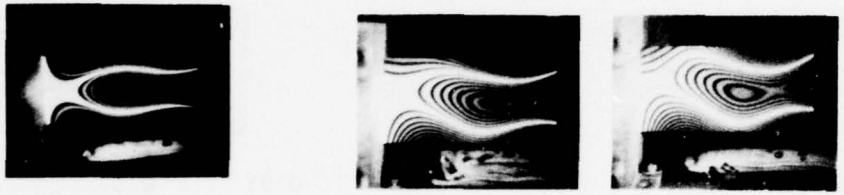

FIGURE 16. ROOT CRACK MODE SHAPES: MODE 7

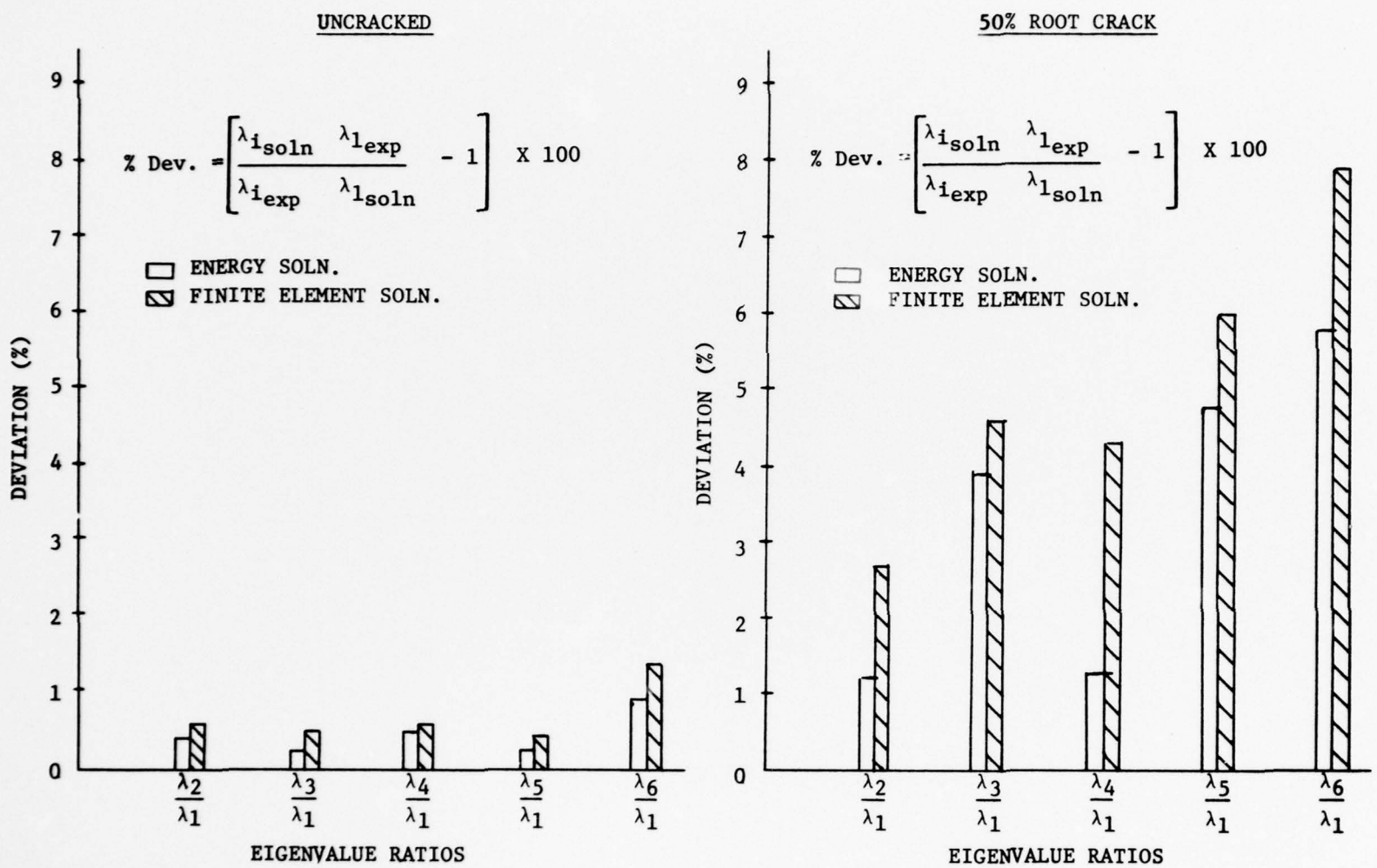

FIGURE 17. EIGENVALUE RATIO DEVIATIONS FROM EXPERIMENTAL SOLUTION

APPENDIX

MATRIX ELEMENTS

$$I1_{ijk\ell} = \frac{(i+2)(i+1)(k+2)(k+1)}{(i+k+1)(j+\ell+1)}$$

$$I2_{ijk\ell} = \frac{(j)(j-1)(\ell)(\ell-1)}{(i+k+5)(j+\ell-3)}$$

$$I3_{ijk\ell} = \frac{(i+2)(i+1)(\ell)(\ell-1)+(j)(j-1)(k+2)(k+1)}{(i+k+3)(j+\ell-1)}$$

$$I4_{ijk\ell} = \frac{(j)(i+2)(\ell)(k+2)}{(i+k+3)(j+\ell-1)}$$

$$I5_{ijk\ell} = \frac{(i+2)(i+1)(k+2)(k+1)}{(i+k+1)}$$

$$I6_{ijk\ell} = \frac{(i+2)(i+1)(\ell)(k+2)(k+1)}{(2)(i+k+1)} + \frac{(j)(i+2)(i+1)(k+2)(k+1)}{(2)(i+k+1)}$$

$$I7_{ijk\ell} = \frac{(j)(i+2)(i+1)(\ell)(k+2)(k+1)}{(i+k+1)\ (3)}$$

$$I8_{ijk\ell} = \frac{(j)(i+2)(\ell)(k+2)}{(i+k+3)}$$

PRECEDING PAGE BLANK-NOT FILMED

$$I9_{ijk\ell} = \frac{(i + 2)(i + 1)(k + 2)(k + 1)}{(i + k + 1)(\ell + 1)}$$

$$I10_{ijk\ell} = \frac{(j)(i + 2)(i + 1)(k + 2)(k + 1)}{(i + k + 1)(\ell + 2)}$$

$$I11_{ijk\ell} = \frac{(i + 2)(i + 1)(\ell)}{(i + k + 3)}$$

$$I12_{ijk\ell} = \frac{(j)(i + 2)(i + 1)(\ell - 1)}{(i + k + 3)}$$

$$I13_{ijk\ell} = \frac{(j)(i + 2)(k + 2)}{(i + k + 1)(j + 1)}$$

$$I14_{ijk\ell} = \frac{(i + 2)(i + 1)(k + 2)(k + 1)}{(i + k + 1)(j + \ell + 1)}$$

$$I15_{ijk\ell} = \frac{(j)(j - 1)(\ell)(\ell - 1)}{(i + k + 5)(j + \ell - 3)}$$

$$I16_{ijk\ell} = \frac{(i + 2)(i + 1)(\ell)(\ell - 1) + (j)(j - 1)(k + 2)(k + 1)}{(i + k + 3)(j + \ell - 1)}$$

$$I17_{ijk\ell} = \frac{(i + 2)(j)(k + 2)(\ell)}{(i + k + 3)(j + \ell - 1)}$$

$$J1_{ijk\ell} = \frac{1}{(i + k + 5)(j + \ell + 1)}$$

$$J2_{ijk\ell} = \frac{1}{(i + k + 5)}$$

$$J3_{ijk\ell} = \frac{\ell + j}{(i + k + 5)(2)}$$

$$J4_{ijk\ell} = \frac{j \cdot \ell}{(i + k + 5)(3)}$$

$$J5_{ijk\ell} = \frac{1}{(i + k + 5)(\ell + 1)}$$

$$J6_{ijk\ell} = \frac{j}{(i + k + 5)(\ell + 2)}$$

$$J7_{ijk\ell} = \frac{1}{(i + k + 5)(\ell + j + 1)}$$

$$K1_{ijk\ell} = I1_{ijk\ell} + AR_1^4 \cdot I2_{ijk\ell} + \nu AR_1^2 \cdot I3_{ijk\ell} + 2AR_1^2(1 - \nu)I4_{ijk\ell} +$$

$$\alpha \cdot I5_{ijk\ell} + \alpha^2 \cdot I6_{ijk\ell} + \alpha^3 \cdot I7_{ijk\ell} +$$

$$2\alpha^2 \cdot AR_1 AR_2 (1 - \nu) I8_{ijk\ell}$$

APPENDIX (CONTINUED)

$$K2_{ijk\ell} = \alpha \cdot I9_{ijk\ell} + \alpha^2 \cdot I10_{ijk\ell} + \nu AR_1 AR_2 \cdot I11_{ijk\ell} + \alpha \cdot AR_1 AR_2 \nu \cdot I12_{ijk\ell} + 2\sigma \cdot AR_1 AR_2 (1 - \nu) I13_{ijk\ell}$$

$$K3_{ijk\ell} = \alpha \cdot I14_{ijk\ell} + AR_1 AR_2^3 \cdot I15_{ijk\ell} + \nu AR_1 AR_2 \cdot I16_{ijk\ell} + 2(1 - \nu) AR_1 AR_2 \cdot I17_{ijk\ell}$$

$$M1_{ijk\ell} = J1_{ijk} + \alpha \cdot J2_{ijk\ell} + \alpha^2 \cdot J3_{ijk\ell} + \alpha^3 \cdot J4_{ijk\ell}$$

$$M2_{ijk\ell} = \alpha \cdot J5_{ijk\ell} + \alpha^2 \cdot J6_{ijk\ell}$$

$$M3_{ijk\ell} = \alpha \cdot J7_{ijk\ell}$$

LIST OF REFERENCES

1. Leissa, A. W., Vibration of Plates, NASA SP-160, N67-62660, 1969.

2. Ritz, W., Gesommelte Werke, Societe Soisse de Physique, Paris, 1911.

3. Szilard, R., Theory and Analysis of Plates, Prentice Hall Pub, Inc., Englewood Cliffs, New Jersey.

4. Bailey, C. D., "Application of Hamilton's Law of Varying Action," AIAA Journal, Vol 13, pp. 1154-1157, September 1975.

5. Bailey, C. D., "A New Look at Hamilton's Principle," Foundation of Physics, Vol 5, No. 3, pp. 433-451, September 1975.

6. Beres, D. P., "Vibration Analysis of a Completely Free Elliptical Plate," Journal of Sound and Vibration, Vol 34, No. 3, pp. 441-443, June 8, 1974.

7. Bailey, C. D., "Hamilton, Ritz and Elastodynamics," ASME Journal of Applied Mechanics, Vol 43, No. 4, pp. 684-688, December 1976.

8. Bailey, C. D., "Exact and Direct Analytical Solutions to Vibrating Systems with Discontinuities," Journal of Sound and Vibration, Vol 44, pp. 15-25, January 1976.

9. Hamilton, W. R., "On a General Method in Dynamics," Philosophical Transactions of the Royal Society of London, Vol 124, pp. 247-308, 1834.

10. Anderson, D. A., "Modeling of Gas Turbine Engine Compressor Blades For Vibration Analysis," AIAA Journal of Aircraft, Vol 12, No. 4, pp. 357-359, April 1975.

☆U.S.Government Printing Office: 1977 — 757-080/165